Molecular mechanism of natriuretic peptide secretion and adaptation to disease in animal model and clinical practice

Doctoral theses

Tímea Kováts, MD

Semmelweis University
Doctoral School of Theoretical Medical Sciences

PhD supervisor: Miklós Tóth, MD, PhD, DSc

Opponents: Barna Vásárhelyi, MD, PhD
István Szokodi, MD, PhD

Doctoral rigolosum, chairman: Zsolt Radák, PhD, DSc
Doctoral rigolosum, members: Andrea Székely, MD, PhD
Endre Zima, MD, PhD

Budapest
2008

I. Introduction

Cardiac natriuretic peptides (atrial natriuretic peptide: ANP, B-type natriuretic peptide; BNP) play an important role in cardiovascular homeostasis through their effects on vasodilatation, natriuresis, diuresis, the renin-angiotensin-aldosterone system and cellular proliferation. Prior to secretion, natriuretic peptides are stored as inactive pro-hormones (pro-ANP and pro-BNP) in the perinuclear granules of cardiomyocytes. Upon secretion, the multi-domain transmembrane serine protease corin cleaves pro-ANP (and probably pro-BNP as well) to generate the active hormone C-terminal ANP (and BNP) and the biologically inactive N-terminal fragment NT-proANP (and NT-proBNP). The main trigger for natriuretic peptide secretion is cardiac wall stretch, although several bioactive agents, such as endothelin, increases natriuretic peptide expression and exocytosis. The natriuretic peptide system is up-regulated during development of heart failure, left ventricular dysfunction, and acute coronary syndromes as well as in other cardiac conditions. As such, the measurement of natriuretic peptide fragments, especially NT-proBNP, provides important diagnostic and prognostic information in the clinical practice. In addition to its diagnostic value, the natriuretic peptide system is a target for therapeutic interventions.

Despite the numerous studies (there are more than 20000 articles published on natriuretic peptides to date) and the importance of natriuretic peptides in health and disease, there are still several questions about the molecular mechanisms controlling natriuretic peptide secretion and processing that remained unanswered. Revealing the details of the molecular mechanisms controlling natriuretic peptide secretion and pro-hormone activation might create the base for further therapeutic modifications of the natriuretic peptide system in several cardiovascular disease affecting millions, such as heart failure and hypertension.

II. Aims

1. In vitro and ex vivo studies: physiologic mechanism of ANP secretion from cardiomyocytes

A. Regulation of ANP secretion from cardiomyocytes

SNARE molecules and SNARE related peptides, such as the munc18 molecules are widely studied regulators of vesicle trafficking and membrane fusion in other secretory cells. Our aim was to investigate whether ANP secretion proceeds through a SNARE-dependent mechanism, and whether munc18c, a well-known regulator of SNARE complex formation, controls ANP secretion from cardiomyocytes.

B. Characterization of corin, the pro-ANP convertase

Corin, the enzyme responsible for pro-ANP activation by a specific proteolytic cleavage, was recently identified. Although corin has been shown to be abundantly expressed in the heart, its cellular localization was unknown. Corin cDNA sequence had also predicted that corin is synthetised as a zymogen, pro-corin, and needs proteolytical clevage for activation. To address these issues, our aim was to investigate the cardiac localization and posttranslational modification and molecular forms of corin.

2. In vivo studies: natriuretic peptide secretion in animal model of diabetes combined with cardiac hypertrophy

Diabetes mellitus is associated with several cardiovascular diseases. Natriuretic peptides and endothelin are counterregulatory hormones involved in the cardiovascular complications of diabetes mellitus. Although there are numerous reports on these changes in the basal state, little is known about the responses to increased acute hemodynamic burden in diabetes. The aim of our experiments was to characterize the changes of ANP and endothelin secretion in response to acute hemodynamic load in experimental diabetes.

3. Clinical practice: natriuretic peptide secretion in bradycardia

Increased natriuretic peptide secretion due to tachycardia-related cardiomyopathy is a well-known phenomenon in clinical practice. The cellular mechanism behind the increased secretion is myocardial stretch. However, not only tachycardia, but bradycardia might lead to increased cardiac wall tension. Our aim was to investigate whether bradycardia might manifest in clinically significant elevation of natriuretic peptide serum level, and whether cessation of the arrhytmia results in a reduction of the NP level.

lll. Methods

1. Cloning, bacterial expression, and purification of bacterial proteins

Recombinant mouse corin fragments, stem domain and protease domain with activation peptide, were generated in bacterial systems. Briefly, the coding regions of corin were cloned by PCR from a total mouse heart cDNA library into pCR™ II vector. The confirmed cDNAs were ligated into the pGEX-4T-2 or the pProEX-HTb vector.
The constructs were verified and the GST-tagged proteins were expressed in *Escherichia coli* strain BL21. The proteins were solubilized from inclusion bodies, refolded and dialyzed. The GST tag was cleaved with thrombin. One of the protease domain construct was expressed as a His_6-tagged protein. All the proteins were analyzed by SDS-PAGE and Western blotting.

2. Antibodies

Anti-ANP serum directed against C-ANP, polyclonal anti-syntaxin 2 and syntaxin 4, monoclonal anti-syntaxin 4 and monoclonal anti-syntaxin 6 antibodies were available commercially.

A, Polyclonal antibody generation

After obtaining preimmune serum, New Zealand white rabbits were subcutaneously immunized with 50 to 100 μg of purified proteins emulsified in Freund's adjuvant every 2 weeks over 3-4 months, and blood samples were taken to monitor antibody production. The specificity of the polyclonal serums was tested against the original immunizing antigens and mouse heart tissue and other tissues extracts by Western blotting.

B, Monoclonal antibody generation

Female BALB/c mice were immunized intraperitoneally with 50 μg of recombinant protein in complete Freund's adjuvant and two weeks later were given booster injections. The antibody titer was determined by solid phase radioimmunoassay (RIA). Spleenocytes were fused with murine SP2/0 cell line. Hybridomas supernatants were tested for the production of MAbs by solid phase RIA, and antibody specificity was tested by immunoblotting. Hybridomas were cloned by limiting dilution and sub-cloned. MAbs have been classified and sub-classified by ELISA.

3. Protein extraction

A, Protein extraction from tissue

Briefly, tissue was quickly washed in ice-cold phosphate buffered saline (PBS), snap-frozen in liquid nitrogen, and homogenized in TRIS buffer supplemented with complete protease inhibitor cocktail. Tissue homogenates were centrifuged and supernatants rich in cytosolic proteins were saved at -80 ^{o}C. Pellets were washed and centrifuged repeatedly. After washing, pellets rich in membrane proteins were homogenized in a detergent-containing high ionic concentration buffer. Tissue homogenates were incubated for 1 hr at 4 ^{o}C with shaking, followed by centrifugation. Supernatant was collected and saved at -80^{o}C until further analysis. Protein concentration of extracts was measured by the BCA Protein Assay Kit.

In separate experiments, contracting mouse hearts (left ventricle) were injected *in situ* with 1 μM FITC-Phe-Pro-Arg-chloromethyl ketone (FITC-FPR-CMK) in PBS, incubated for 5 min and harvested. Membrane-bound proteins were extracted according to the protocol above.

B, Protein extraction from cultured cells

Cultured neonatal atrial cardiomyocytes and HL-1 cells were incubated for 1 h at 4 ^{o}C in 50 mM Tris-HCl buffer containing 125 mM NaCl, 1% Triton X-100 and protease inhibitor cocktail and centrifuged. The protein concentration of the supernatant was determined by the BCA Protein Assay Kit.

4. Plasma peptide extraction and radioimmunoassay

Acidified plasma (1.5 mL) was applied to Sep Pack C18 cartridges previously activated by methanol and 0.1 % trifluoroacetate, and eluted with 80% acetonitrile in 0.1% trifluoroacetate buffer. Eluates were evaporated and reconstituted with radioimmunoassay buffer. Immunoreactive peptide concentrations (NT-proANP, ET-1) were determined with radioimmunoassays. Intra-assay and interassay coefficients of variation were lower than 10% and 15%, respectively.

5. Concanavalin A-Sepharose binding assay and cell surface labeling

Cell lysates (5.5 μg/ml) prepared as described above were incubated with one-fifth volume of Concanavalin A-Sepharose for 1.5 h at 4 ^{o}C according to the manufacturer's protocol. HL-1 cells were incubated in PBS containing 1 mg/ml EZ-Link^{TM} Sulfo-NHS-LC-Biotin. The excess of EZ-Link^{TM} Sulfo-NHS-LC-Biotin was captured by incubation with 50 mM TRIS-HCl. After washing, cells were lysed, and lysates were incubated with Immobilized Streptavidin. Bound and unbound fractions were analyzed by Western blotting.

6. Western-blotting

Following denaturation by boiling in Laemmli sample buffer, samples were subjected to SDS-PAGE and electroblotted. Non-specific binding sites were blocked by incubation with 5% skim milk. After incubation with various primary antibodies (as indicated), secondary goat anti-rabbit/or goat anti-mouse (IgG + IgM) alkaline phosphatase-labeled antibody was used for detection. Immunoreactivity was visualized with ECF (enhanced chemifluorescence) substrate by fluorescence/phosphoimager. To analyze other components, immunoblots were sometimes stripped of initial antibodies by incubation in stripping buffer (100 mM β-mercapto-ethanol, 62.5 mM TRIS-HCl, 2% sodium-dodecyl-sulfate) at 50 ^{o}C with occasional gentle shaking. Following incubation, membranes were washed until traces of β-mercapto-ethanol was removed. Then membranes were blocked in 5% skim milk. Prior to additional immunoblot analysis, the blots were shown to be

without immunoreactivity by developing them with enhanced chemifluorescence detection system and analysis by phosphorimaging.

7. Immunoprecipitation

Heart extracts rich in membrane-bound proteins were pre-cleared by incubation with protein A agarose or protein G Sepharose 4B. Purified polyclonal antibodies or rabbit IgG were coupled to protein A agarose slurry. Similarly monoclonal antibodies were coupled to G Sepharose 4B slurry. Pre-cleared protein extract was immunoprecipitated by incubation with antibody-coupled beads. Immunoprecipitates were washed with ice-cold PBS, boiled in sample buffer, and centrifuged. Supernatants were analysed by SDS-PAGE followed by immunoblotting as described above.

8. Cardiomyocytes and HL-1 cell culture

Neonatal rat atrial and ventricular cardiomyocytes were isolated and cultured separately by the Worthington Neonatal Cardiomyocyte Isolation System Kit according to the manufacturer's protocol. From day 2. cells were cultured in modified Complete Serum-Free Media (CSFM that contains: DMEM/F12, 25 mM HEPES, 1.7 μM insulin, 1 μM transferrin, 10 nM sodium-selenite, 1 nM tri-iodo-thyronine, 0.2% BSA, 190 nM dexamethasone, 1 mg/l arachidonic acid, 0.5 mg/ml docosahexanoic acid, and 100 Unit/ml penicillin/streptomycin).

The murine cardiomyocyte-like cell line HL-1 was kindly provided by Dr. William C. Claycomb. Cells were cultured in Claycomb medium supplemented with 10% fetal bovine serum, 100 μg/ml penicillin/streptomycin, 0.1 mM norepinephrine and 2 mM L-glutamine.

9. Immunofluorescence staining

Cardiomyocytes were grown on an 8-well glass chamber slide and prepared for immunofluorescence by washing followed by fixation. Cells were permeabilized with 0.1% Triton-X100 or 0.1% saponin. Non-specific binding sites were blocked and primary

antibodies were applied. After repeated washing, primary antibodies were detected by Alexa Fluor 488-labeled goat anti-mouse or Alexa Fluor 594-labeled goat anti-rabbit secondary antibodies. Nuclei were visualized by staining with 4',6'-diamidino-2-phenylindole hydrochloride. Slides were mounted with Prolong Antifade Kit and analysed with an LSM 510 Meta Confocal Microscope. Localization of labeled proteins was analyzed using Axion vision software.

10. Cell permeabilization, secretion assay and ANP measurement

Atrial or ventricular neonatal cardiomyocytes were used for secretion assay on culture day 7-9. Streptolysin-O (SLO) was dissolved in 0.05% BSA, reduced with dithiothreitol on ice, aliquoted and stored at -80 ^{o}C. Cells were briefly rinsed with an intracellular Ca^{2+}-buffering solution (KG buffer), then incubated in KG buffer containing SLO and various antibodies. Secretion was induced by priming the samples with Na_2ATP, Na_2GTP and increasing the free Ca^{2+} concentration up to ~100 μM. The free Ca^{2+} concentration was determined by the WinMaxc v2.05 software and titration curves. Supernatants were collected and then stored at -80^{o}C until samples were analysed. Cells were lysed in 1% Triton-X100 followed by centrifugation. Supernatants were collected and saved at -80^{o}C until further evaluation. Immunoreactive ANP was measured with a c-ANP ELISA kit. The percentage of permeabilization was assessed with a colorimetric lactate dehydrogenase (LDH) assay kit.

11. Flow cytometry analysis

HL-1 cells were cultured in 6-well plates under conditions described above. Non-permeabilized cells were washed with ice-cold PBS containing 3% fetal bovine serum, collected, centrifuged, resuspended at a density of $4x10^6$ cells/ml and stained with anti-corin pooled or non-specific control pooled MAbs. After repeated washing and blocking, cells were stained with Alexa Fluor 488-labeled goat anti-mouse IgG/IgM. Cells were washed and fixed with BD Cytofix buffer. Fluorescence was measured in a flow cytometer with CellQuest software for acquisition and analysis**.**

12. Diabetes induction and arterio-venous shunt preparation in dogs

Mongrel dogs from each sex were randomly assigned for the diabetic or the metabolically healthy group. Diabetes was induced by a single infusion of alloxan-monohydrate. Dogs were investigated 8 weeks after the induction of diabetes.
Arterio-venous shunt was prepared as a modell of acute hemodynamic load in each group. General anaesthesia was induced and maintained by sodium pentobarbital. A section of 3-4cm shunt was placed in both distal femoral regions, between the femoral vein and artery. Control animals were sham operated. Dogs were sacrificed on postoperative day 1 or 3. Samples of peripheral and coronary sinus blood and pericardial fluid were collected, and plasma was separated and frozen at -25^{o}C until further evaluation. Blood pressure was measured in the abdominal aorta. Hearts were harvested and weighed.

13. Statistics

Differences between multiple groups were assessed by an analysis of variance with a 1) Bonferroni-Dunn correction for multiple statistical inferences (in tissue culture studies); 2) Mann-Whitney test (in animal models of cardiac load and diabetes). In corin studies, statistical analysis was performed by paired *t*-test. A $P < 0.05$ was considered to be statistically significant. Error bars represent standard deviations. Results represent at least three independent experiments.

14. Animals

All studies were performed in accordance with the *Guide for the Care and Use of Laboratory Animals* published by the US National Institutes of Health (NIH Publication No. 85-23, revised 1996), and all procedures were approved by the responsible institutional animal care and use committee.

IV. Results

1. Natriuretic peptide secretion from cardiomyocytes is regulated by munc18c

A, Syntaxin 4 and munc18c colocalize and interact at the plasma membrane of cardiomyocytes

Double immunostaining of primary rat cardiomyocytes showed that munc18c antibody predominantly labeled the plasma membrane of ANP-positive cardiomyocytes (Fig. 1A). Immunoblot analysis revealed that munc18c was expressed in both atrial and ventricular tissues at the predicted relative molecular mass of 67 kDa. Immunostaining localized syntaxin 4 (Fig. 1B) to the plasma membrane in ANP-positive cells. It was also readily detected by immunoblotting in both atria and ventricular lysates as a single band with a relative mass of ~36 kDa. Co-immunoprecipitation studies showed munc18 – syntaxin 4 interaction when probed by a pan-anti-munc18 antibody. Further investigation by a munc18c specific antibody verified munc18c – syntaxin 4 binding.

Syntaxin 6 was detected in a perinuclear pattern, that partially colocalized with ANP (Fig. 1C). Immunoblotting studies demonstrated that syntaxin 6 was present in both atrial and ventricular tissues at an expected relative molecular mass of ~34 kDa. Co-immunoprecipitation demonstrated no munc18 – syntaxin 6

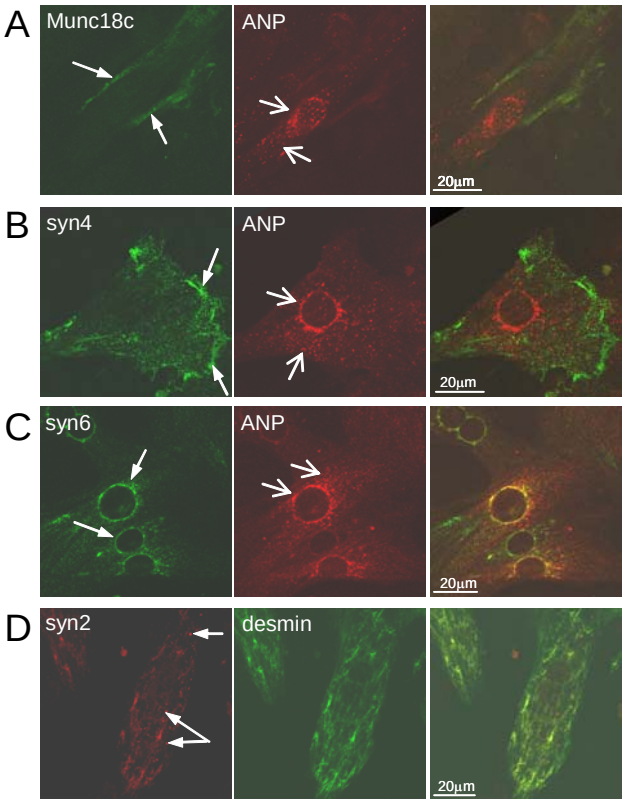

Fig.1. Double immunofluorescence staining of cardiomyocytes

interaction.

Syntaxin 2 (Fig. 1D) was detected in a diffuse granular pattern within the cytoplasm. Co-expression within cardiomyocytes was confirmed by double immunostaining with desmin (Fig. 1D). Syntaxin 2 was detected as a single band of relative mass ~34 kDa in both atrial and ventricular tissues. Co-immunoprecipitation studies revealed only some munc18 – syntaxin 2 interaction when immunoblotted by a pan-anti-munc18 antibody. Furthermore, we could not detect syntaxin 2 – munc18c interaction by a munc18c specific antibody.

B, Munc18c inhibitors selectively enhance ANP secretion

A streptolysin-O permeabilized cardiomyocyte system was developed to examine the functional role of munc18c on ANP secretion. When compared to baseline secretion in permeabilized cardiomyocytes, increased Ca^{2+} triggered release of ANP (Fig. 2, $p < 0.01$). Addition of a control monoclonal antibody had no effect on Ca^{2+}-triggered release of ANP. However, the introduction of the anti-munc18c antibody significantly increased Ca^{2+}-triggered release of ANP ($p < 0.05$).

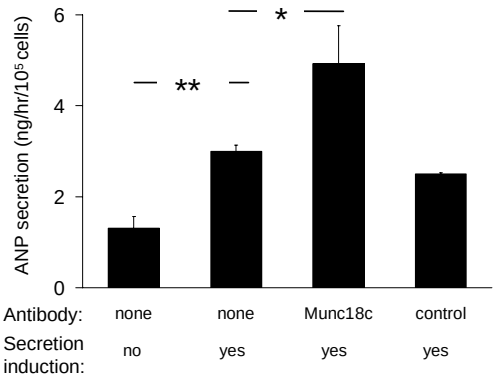

Fig. 2. Inhibition of munc18c increases ANP secretion from permeabilized cardiomyocytes.

2. Pro-natriuretic peptide-convertase corin is localized on the cardiomyocyte surface

A, Expression and localization of native corin protein

In order to investigate native corin on the protein level, as a first step anti-corin rabbit polyclonal antibodies (anti-stem and anti-protease domains) and mouse MAbs (against protease domain) were generated and characterized. Cultured non-permeabilized cardiomyocytes were analyzed by immunofluorescence staining with anti-corin antibodies. Polyclonal anti-corin stem domain antibody and anti-corin protease domain antibody and MAbs localized corin to the plasma membrane surface of cardiomyocytes.

To examine whether native corin is expressed in cardiomyocytes that also express pro-ANP, permeabilized neonatal atrial cardiomyocytes were double stained with mouse anti-corin protease domain MAb and rabbit polyclonal anti-pro-ANP antibodies and analyzed by confocal microscopy. Fig. 3 shows a typically perinuclear, granular staining pattern of pro-ANP (red) and membrane staining of corin (green).

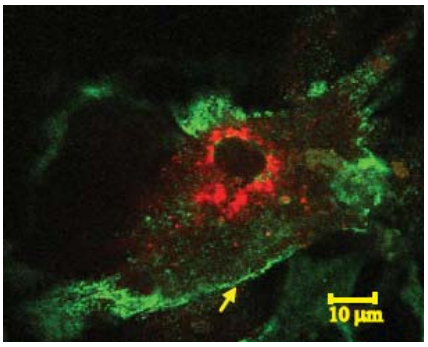

Fig. 3. Double immunofluorescence staining of cardiomyocytes by pro-ANP (red) and corin (green).

B, Molecular size and structure of native corin

The molecular size and structure of native corin was examined in mouse heart extracts in the presence protease inhibitors. Anti-corin protease domain MAbs precipitated corin, which was detected as a 205-210 kDA protein by Western blotting using anti-corin stem domain antibody for detection. Since a 205-210 kDa band was recognized under reducing conditions with both anti-corin stem domain antibody and anti-corin protease domain MAbs, it likely corresponds to full-length corin protein. The discrepancy seen between the

predicted size, 123 kDa and actual molecular mass of corin suggests that the mature corin undergoes post-translational modifications such as glycosylation (analyzed further).

The cDNA sequence predicts that corin is synthesized as a zymogen, pro-corin, and requires proteolytic cleavage to become an active enzyme. Furthermore, corin contains several putative disulfide bonds, upon activation the active corin would remain tethered to the cell-surface by a putative disulfide bond. To determine whether native corin protein is expressed on the plasma membrane surface as a zymogen and/or an active enzyme, Western blotting of the membrane fraction of mouse heart extracts was performed under reducing conditions. The anti-corin stem domain antibody detected corin fragments with relative masses of 180 kDA and 110 kDa. These fragments were not recognized by anti-corin protease domain antibodies and therefore might correspond to structures containing primarily stem domain. The anti-corin protease domain antibody detected corin fragments with relative masses of 45-50 kDa and 90 kDa. These fragments were not recognized by anti-corin stem domain antibody and might correspond to structures containing primarily protease domain. Immunoprecipitation of full-length corin (205-210 kDa) under reducing conditions confirmed that at least a portion of corin in cardiac tissue is the zymogen form. Detection of full-length corin and corin fragments in the membrane fraction of the mouse heart extract suggests that corin is present on the cardiomyocyte surface in both its zymogen (assessed by its inability to be cleaved by mercaptoethanol) and potentially active (cleaved by mercaptoethanol treatment) forms.

To further explore our finding that corin is present on the plasma membrane surface as a catalytically active enzyme, we used an irreversible protease inhibitor, FITC-FPR-CMK, which mimics the corin cleavage sequence in pro-ANP. When FITC-FPR-CMK is injected into the mouse heart, it forms a covalent complex with any active proteases that recognize its sequence. After FITC-FPR-CMK injection, mouse hearts were extracted and the membrane fraction was subjected to SDS-PAGE followed by electro-blotting. The fluorescent FITC-tag on the inhibitor allows for detection of protease-containing covalent complex. Two bands with molecular size around 50 and 90 kDa were detected after fluorescence scanning. The same membrane was then probed with anti-corin protease domain antibody confirming that the fluorescent bands corresponded to corin.

C, Corin expression in cardiomyocyte-like HL-1 cells

The murine HL-1 cell line retains the phenotypic characteristics of the adult cardiomyocyte. The localization of corin on the external plasma membrane of HL-1 cells was confirmed by flow cytometry. To further confirm the membrane-bound extracellular localization of corin, HL-1 cells were surface-labeled with biotin. The labeled cell lysate was separated on Immobilized Streptavidin followed by Western blotting with anti-corin MAbs. Results showed that 205-210 kDa form of corin exhibits affinity toward Streptavidin–Agarose indicating its localization on the external plasma membrane of HL-1 cells.

To explain the discrepancy between the predicted and actual molecular mass of corin we evaluated the glycosylation status of corin. The HL-1 cell extract was separated on Concanavalin A-Sepharose, which binds only glycosylated proteins. Western blotting showed that the 205-210 kDa form of corin exhibits strong affinity toward Concanavalin A–Sepharose indicating its glycosylation. The 110-115 kDa form of corin had reduced glycosylation assessed by its inability to bind Concanavalin A-Sepharose. The glycosylation status of the 205-210 kDa form of corin was further confirmed by separation of the rat neonatal cardiomyocyte extract on Concanavalin A–Sepharose.

3. Acute hemodynamic load increases natriuretic peptide level both in healthy and diabetic dogs

A, Changes in cardiovascular parameters due to acute hemodynamic load in diabetic and metabolically healthy dogs

Mean arterial blood pressure, heart weight, left and right ventricle to body weight ratios were measured in diabetic and healthy dogs, with and without acute hemodynamic load in each group. As a model for acute hemodynamic strain, arterio-venous shunt was used, and cardiovascular parameters were evaluated on the first and third days of operation. Diabetic dogs had significantly lower blood pressure as compared with healthy controls (79±2 mmHg vs. 89±6 mmHg, respectively; $p<0.05$). Acute hemodynamic strain on

postoperative day 1 further decreased the blood pressure in these dogs (72±3 mmHg vs. 79±2 mmHg; $p<0.05$). However, in metabolically healthy dogs shunting did not have any effect on blood pressure. Heart weight/body weight ratio, as well as left and right ventricle to body weight ratios separately, were increased upon shunting, however, there was no difference between the metabolically healthy and the diabetic group.

B, Endothelin levels in healthy and diabetic dogs with normal circulation and after acute hemodynamic load

Endothelin-1 (ET-1) level was measured in the plasma, coronary sinus and pericardial fluid of metabolically healthy and diabetic dogs without and with hemodynamic load. ET-1 level in the peripheral plasma was significantly higher in diabetic dogs than in the healthy controls (Fig. 4A). Shunting did not change ET-1 level in the healthy dogs, but significantly decreased the level in the diabetic group. Similar changes were observed in the coronary sinus (Fig. 4B). However, in the pericardial fluid, ET-1 level was higher than that of the plasma, and neither shunting nor diabetes changed it (Fig. 4C).

C, Acute hemodynamic load increases NT-proANP levels in different compartments of diabetic and healthy dogs

To further investigate the combined effect of altered ET-1 levels and hemodynamic load on natriuretic peptide secretion, we measured NT-proANP levels in the plasma, coronary sinus and pericardial fluid of metabolically healthy and diabetic dogs without and with hemodynamic load (Fig. 5). Levels of NT-proANP showed similar patterns in all three compartments, being comparable under basal conditions but significantly increased upon shunting (Fig. 5A-C). However, elevation on NT-proANP levels due to shunting was higher in the diabetic group than in the metabolically healthy controls.

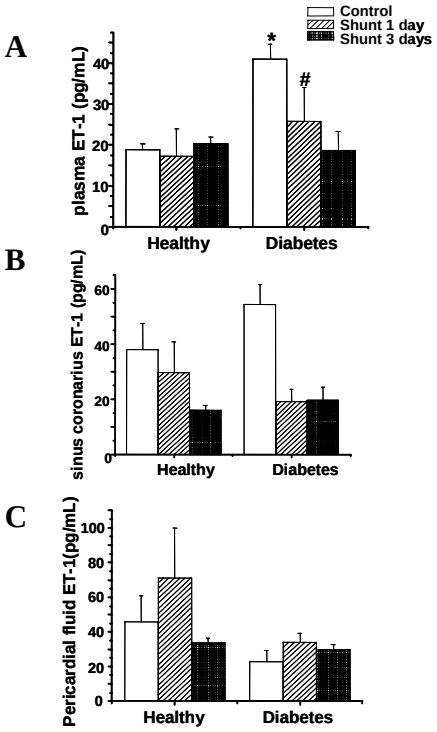

Fig. 4. ET-1 levels in healthy and diabetic dogs with normal circulation and 1 and 3 days after shunting.

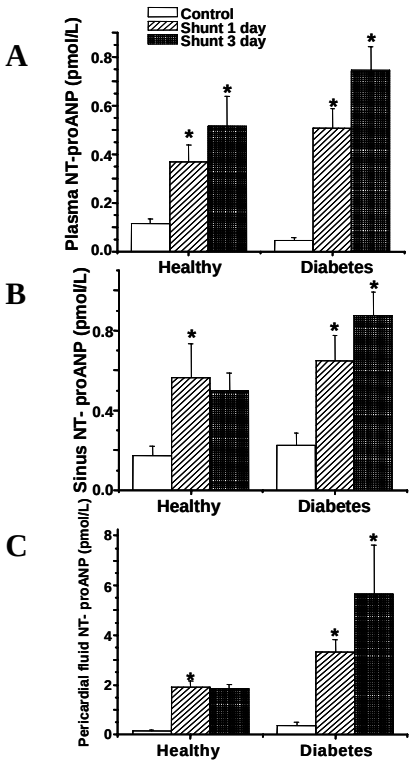

Fig. 5. NT-proANP levels in different comparments of healthy and diabetic dogs with normal circulation and 1 and 3 days after shunting.

4. Bradycardia can induce increased serum natriuretic peptide level

A 94 year-old woman was admitted to the hospital after 4 days of worsening weakness and dyspnea. Her regular medication included beta-blocker (5 mg bisoprolol per day) and thiazide diuretics as antihypertensive therapy. At admission, ECG showed sinus arrest with narrow-QRS complex junctional escape rhythm, with a heart rate of 40 bpm. Routine laboratory tests (including TSH and troponin-T) displayed normal values. However, NT-proBNP serum level was highly increased (22420 pg/ml; normal reference value is below 270 pg/ml). Echocardiographic findings displayed normal systolic ventricular function and mild degenerative mitral and aortic insufficiency.

Beta-blocker therapy was discontinued for assumed therapy-induced bradyarrhythmia. Due to the stabile hemodinamic parameters temporary pacemaker was not implanted.

The patient's bradyarrhythmia resolved in 48 hours and sinus rhythm with 90/min frequency returned. Control NT-proBNP serum level was markedly lower (2117 pg/ml). Free from her actual symptoms the patient was discharged from the hospital.

V. Conclusion

1. Munc18c regulates ANP secretion

The studies above demonstrated that neonatal cardiomyocytes contain the secretory molecules syntaxin 2, 4 and 6, as well as munc18c. Syntaxin 4 and munc18c displayed a pattern of expression consistent with localization to the plasma membrane. In contrast, syntaxin 2 showed a more diffuse granular distribution throughout the cytoplasm of cardiomyocyte. Syntaxin 6 partially co-localized with pro-ANP in peri-nuclear granules, although it was not found in pro-ANP containing granules at the periphery of the cell. The plasma membrane expression pattern of syntaxin 4 and munc18c suggested that these two molecules may interact in the heart and this interaction was confirmed by co-immunoprecipitation studies. In SLO-permeabilized cardiomyocytes systems, pro-ANP secretion was reproducibly induced by increased intracellular Ca^{2+}. Introduction of a munc18c-specific MAb significantly increased Ca^{2+}-triggered secretion of pro-ANP whereas a control MAb had no effect. This provided strong evidence that pro-ANP secretion from cardiomyocytes is modulated by munc18c.

2. Corin is co-expressed with pro-ANP and localized on the cardiomyocyte surface in both zymogen and catalytically active forms

A series of anti-corin polyclonal and monoclonal antibodies directed against the stem and protease domains allowed us to identify for the first time the native corin protein on the cell surface of rat neonatal cardiomyocytes and murine HL-1 cardiomyocyte-like cells by immunofluorescence staining, flow cytometry and biotin cell surface-labeling techniques. Furthermore, we showed that native corin is expressed in cardiomyocytes that also express its substrate, pro-ANP, providing further evidence that corin may contribute to the regulation of the natriuretic peptide system *in vivo* by pro-ANP processing**.** Our finding of both zymogen and active forms of corin in mouse heart suggests that regulation of corin activity might control the ratio between circulating pro-ANP and cleaved ANP. The

zymogen form could be considered as repository for corin on the membrane surface of cardiomyocytes which could be easily activated during periods of increased demand such as increased hemodynamic strain, where an enzymatic cleavage of pro-ANP may play a key role.

3. Cardiac strain reduces ET-1 and increases ANP level in diabetes mellitus

ET-1 plasma and sinus coronarius levels were not influenced by hemodynamic strain in metabolically healthy animals, however, diabetes caused higher basal ET-1 levels which significantly decreased upon shunting. Pericardial fluid contained higher ET-1 level in both metabolically healthy and diabetic animals, and its level did not change due to shunting neither in diabetes nor in the healthy controls. NT-proANP levels in different compartments are increased upon cardiac strain both in diabetes and in metabolically healthy controls, although NT-proANP levels tend to be higher in the diabetic animals. We conclude that 1) the pericardial space behaves as a functionally different compartment for systemic ET-1 level; 2) NT-proANP levels are increased in response to hemodynamic load both in diabetes and in metabolically healthy controls, supporting the value of natriuretic peptide measurement for the diagnosis of acute cardiac strain in diabetes mellitus 3) higher NT-proANP levels in diabetic animals support the need for different cutoff values for diagnostic purposes in diabetes mellitus.

4. Bradycardia can induce increased plasma BNP level

In the case of an elderly woman, we observed extremely elevated natriuretic peptide-level due to bradycardia induced by sinus arrest with a junctional escape rhythm provoked by beta-blocker therapy. Cessation of the medication resulted in sinus rhythm and a rapid decrease of the natriuretic peptide-level. We conclude that not only tachycardia, but bradycardia, or asynchronous contraction might lead to cardiac wall distention, and such as, increased plasma natriuretic peptide level, and elevated natriuretic peptide-levels might indicate subclinical cardiomyopathy induced by bradycardia.

VI. List of publications

1. Related

Kováts T and Tomcsányi J: Bradycardia and B-type natriuretic peptide. Int J Cardiol. IJC-D-08-00826 In press.

Gladysheva IP, Robinson BR, Houng AK, Kováts T and King SM: Corin is co-expressed with pro-ANP and localized on the cardiomyocyte surface in both zymogen and catalytically active forms. J Mol Cell Cardiol. 2008 Jan;44(1):131-42.

Kováts T, Wettstein A, Nagy E and Tomcsányi J: Bradycardia can induce increased serum natriuretic peptide-level. Int J Cardiol. 2008 Jan 11;123(2):e43-4.

Skoumal R, Seres L, Soós P, Balogh E, Kováts T, Rysa J, Ruskoaho H, Tóth M and Horkay F: Endothelin Levels in Experimental Diabetes Combined with Cardiac Hypertrophy. J Cardiovasc Pharmacol. 2004 Nov;44:S195-S197.

2. Unrelated

Pósa I, Horkay F, Seres L, Skoumal R, Kováts T, Balogh E, de Chatel R, Tóth M and Kocsis E: Effects of Experimental Diabetes on Endothelin-induced Ventricular Arrhythmias in Dogs. J Cardiovasc Pharmacol. 2004 Nov;44:S380-S382.